

## Diffusion on loopless critical percolation cluster

This article has been downloaded from IOPscience. Please scroll down to see the full text article.

1995 J. Phys. A: Math. Gen. 28 291

(<http://iopscience.iop.org/0305-4470/28/2/007>)

View [the table of contents for this issue](#), or go to the [journal homepage](#) for more

Download details:

IP Address: 171.66.16.68

The article was downloaded on 02/06/2010 at 00:39

Please note that [terms and conditions apply](#).

# Diffusion on loopless critical percolation cluster

Sonali Mukherjee†, Donald J Jacobs‡ and Hisao Nakanishi†

† Department of Physics, Purdue University, W Lafayette, IN 47907, USA

‡ Institute for Theoretical Physics, State University, Princetonplein 5, PO Box 80006, 3508 TA Utrecht, The Netherlands

Received 25 August 1994, in final form 26 October 1994

**Abstract.** In this paper, we calculate the dynamical exponents of diffusion,  $d_w/d_f$  and  $d_s$ , on a percolation cluster at  $p_c$  with no loops, for the square and simple cubic lattices by the method of spectral analysis of the transition probability matrix. Results show that  $d_s$  varies significantly with the spatial dimension, unlike in conventional percolation, but the Alexander–Orbach scaling relation  $d_s = 2d_f/d_w$  still holds. Thus it rules out the possibility that this scaling relation fails for all loopless fractals because of trapping.

## 1. Introduction

The study of diffusion on fractals is important because it gives deeper insight into many physical processes such as electrical transport in disordered composites [1,2] and fluid flow in porous media. Besides these applications it is also interesting to look at the way in which fundamental physical processes like diffusion are modified by the intricate geometrical properties of a fractal, as reflected in the non-integral fractal dimensionality.

It is well established that the mean square displacement of a random walk on a fractal in the asymptotic long-time limit is given by a power law

$$\langle R(t)^2 \rangle \sim t^{2/d_w} \quad (1)$$

where  $\langle R(t)^2 \rangle$  is the mean square displacement of a  $t$ -step random walk and  $d_w$  is the walk dimension. In a regular ordered lattice  $d_w = 2$ , and equation (1) reduces to the well known linear relation between the mean square displacement and time. On a fractal substrate,  $d_w$  is greater than 2, making the mean square displacement depend sublinearly on time. It is also well known that the return-to-starting-point probability of the random walk,  $P(t)$ , in the long-time limit obeys the power law

$$P(t) \sim t^{-d_s/2} \quad (2)$$

where  $d_s$  is called the spectral dimension of the walk. In a regular ordered substrate,  $d_s$  equals the embedding space dimension,  $d$ , but in a fractal medium  $d_s < d$ , because progressive displacement of the random walker further from the starting point is hampered by its encounter with the irregularities of the medium.

The Alexander and Orbach scaling law [3]

$$d_s = 2d_f/d_w \quad (3)$$

which relates the dynamical exponents  $d_w$  and  $d_s$  to the static exponent  $d_f$  (fractal dimension of the fractal) was initially believed to hold true for random walks on all types of fractals.

Evidence for the breakdown of this scaling relation on tree-like structures was first given by Dhar and Ramaswamy [4] on Eden trees in two dimensions (see also Nakanishi and Herrmann [5]). It was also recently shown [6] not to hold on the diffusion-limited aggregate (DLA), which is essentially loopless on large scales.

All the above facts seem to suggest that diffusion on loopless fractals falls into a qualitatively different category from diffusion on fractals with loops on large length scales. Due to the absence of loops the walker gets trapped and is not able to explore the asymptotic fractal nature of the underlying structure, which is required for the Alexander–Orbach scaling law to hold true. It is important to put this conjecture on a firmer foundation, since tree-like fractals often result from irreversible growth processes. For instance, tree-like fractals are formed during various physical processes like dielectric breakdown [7, 8], colloidal aggregation [9], dendritic growth [10] and fluid–fluid displacement [11].

In this paper, we try to further our understanding of diffusion on tree-like structures by testing the Alexander–Orbach scaling relation on a different type of loopless fractal, namely the loopless percolation cluster. Percolation with loop suppression was first studied by Tzschichholz *et al* [12]. However, the authors of [12] studied the effects of the removal of loops from the percolation cluster by calculating the walk exponent  $d_w$ , and used the Alexander–Orbach scaling relation to determine the other dynamical exponent  $d_s$ , without questioning the validity of the scaling relation.

A conventional way to make a site percolation cluster is a variant of the breadth-first search [13], where one starts from a seed site which is occupied and then considers each nearest neighbour of this site for potential occupation with probability  $p$ . If a neighbouring site is chosen for occupation, it is added to the cluster and a *primary* link is established with the existing cluster. As this process continues and the cluster grows, it may happen that a neighbouring site is occupied and so it is already part of the cluster. Ordinarily if such a neighbour exists, then a *secondary* link is established between it and the site whose neighbours are currently being searched. We have ensured the looplessness of the cluster by suppressing these secondary links without altering the geometry (position of all sites) of the cluster. Consequently the  $p_c$  and the static exponents of our cluster are *exactly* the same as those of the conventional critical percolation cluster. We term the cluster which is formed by such an algorithm a *loopless site percolation* cluster. So the essential difference between the conventional and loopless site percolation cluster is that, in the former case, all occupied nearest neighbours of the underlying lattice are linked, whereas all the secondary links are cut in the latter case. An example of loopless percolation cluster is shown in figure 1.

It should be noted that our model of a loopless percolation cluster is different from that of [12]. In the latter work, while making the cluster, they blocked those growth sites which had the potential to form loops. Thus the location of the sites of the ensuing loopless percolation cluster are changed from those of the conventional percolation cluster, which makes it necessary to determine the  $p_c$  and the static exponents of the loopless cluster. In particular, in their case, the identification of  $d_f$  with that of conventional percolation was subject to (numerical) verification. In our case, this is automatic and exact.

In this paper we are dealing with a two-step process. First we make the loopless percolation cluster and then perform the random walk on it. Since the fractal clusters in this case are statistical, we then perform a quenched average over the disorder. This process involves calculating the quantities of interest on each member of an ensemble of independent configurations and then taking the average over these.

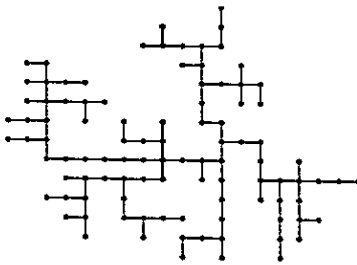


Figure 1. A loopless percolation cluster of 100 sites where permitted links among the sites are shown.

## 2. Spectral analysis

We first define the transition probability matrix and then give the connection between its eigenvalues and the dynamical exponents of the random walk,  $d_s$  and  $d_w/d_f$ . We also give a short discussion on the method used in the diagonalization of  $\mathbf{W}$ .

The matrix  $\mathbf{W}$  is such that an element  $W_{ij}$  gives the probability that the random walker jumps from site  $j$  to site  $i$ .  $W_{ij}$  is either zero (corresponding to those sites  $j$  which are not linked to site  $i$ ), or a positive number (corresponding to the probability of jumping to the linked nearest neighbour). Also, the sum of all the elements of any column of  $\mathbf{W}$  is 1, corresponding to conservation of the particle probability. The above two properties makes the matrix  $\mathbf{W}$  a Markov matrix. As with all Markov matrices,  $\mathbf{W}$  has the eigenvalue 1 corresponding to the stationary state.

For the sake of simplicity the random walk on the cluster is subject to the ‘blind ant rule’, since the exponents obtained are not sensitive to the rule selected within the same universality class. According to the blind ant rule, the random walk has an equal jumping probability of  $1/z$  to an available nearest neighbour, where  $z$  is the coordination number of the underlying lattice, and stays at its current site with the probability of  $1 - w/z$  (where  $w$  is the number of linked neighbours of the current site).

All the information about the geometrical and in particular the fractal nature of the cluster is contained in the location of the non-zero elements of  $\mathbf{W}$ , and the numerical values of elements of  $\mathbf{W}$  are dictated by the transition rules of the random walk. It is possible to extract the dynamical exponents characterizing the random walk from the spectrum of  $\mathbf{W}$ . In particular the exponent  $d_s$  may be obtained from the power-law behaviour of the density of eigenvalues of  $\mathbf{W}$  in the limit that  $\lambda$  tends to unity [14]

$$n(\lambda) \sim |\ln \lambda|^{(d_s/2)-1} \tag{4}$$

where  $\lambda$  is an eigenvalue of  $\mathbf{W}$  and  $n(\lambda)$  is the density of eigenvalues.

The timescale associated with the decay of an eigen-mode is given by  $|\ln \lambda|^{-1}$ . The slowest-decaying eigen-mode which is of interest is the mode corresponding to the second-highest eigenvalue  $\lambda_2$ . The timescale  $t_2$  corresponding to this mode should characterize the timescale for the random walk to travel just enough to explore the entire cluster. This is reflected in the fact that the eigenvector corresponding to  $\lambda_2$  has its non-zero components spread out over the entire cluster. Thus the root-mean-square distance  $R$  travelled in time  $t_2$  must be related to the size of the cluster  $S$  by  $R \sim S^{1/d_f}$ . From this and equation (1), we

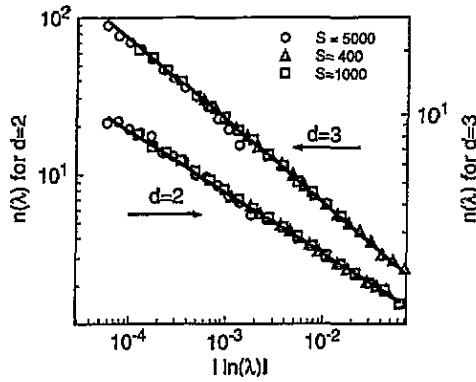


**Figure 2.** Density of eigenvalues  $n(\lambda)$  normalized by the cluster size for the blind ant against  $|\ln \lambda|$  on logarithmic scales. The upper curve corresponds to  $d = 3$  and the lower to  $d = 2$ . The symbols  $\Delta$ ,  $\square$  and  $\circ$  correspond to cluster sizes 400, 1000 and 5000, respectively.

**Table 1.** Size and number of clusters used in the disorder averaging for  $n(\lambda)$  and  $\lambda_2$ .

$d$	Cluster size	Number of clusters
2 (square lattice)	400	2899
	1000	4500
	5000	4250
3 (simple cubic lattice)	400	2000
	1000	3000
	5000	2000

arrive at the following finite-size scaling law:

$$|\ln \lambda_2| \sim S^{-d_w/d_f}. \quad (5)$$

Numerical results supporting this scaling for ordinary percolation were given in [14], and for DLA in [6].

The eigenvalues near unity are of interest because they determine the asymptotic long-time behaviour of the random walk dynamics. Therefore it is necessary to calculate accurately the top-lying eigenvalues near unity, but not the entire eigenspectrum of  $\mathbf{W}$ . In this work we have used the Arnoldi–Saad algorithm to diagonalize  $\mathbf{W}$ . In this algorithm a smaller subspace containing the information about the eigenvalues near unity is extracted from the original  $\mathbf{W}$ , allowing this subspace to be diagonalized exactly and efficiently [14].

In figure 2 the density of eigenvalues per site  $n(\ln \lambda)$  is plotted against  $|\ln(\lambda)|$  on logarithmic scales in  $d = 2$  and  $d = 3$ . It is calculated by binning the eigenvalues obtained from the ensemble of clusters in logarithmic bins and then dividing it by the size of the cluster, the binwidth and the number of clusters. The number of clusters over which the ensemble average is taken and the corresponding cluster sizes are given in table 1.

Figure 2 shows the data collapse for the clusters of different sizes. The symbol sizes are larger than the statistical fluctuations. From the slope of the above plot the value of  $(d_s/2) - 1$  can be obtained for two and three dimensions. The lines over the data are drawn with slopes equal to the estimated value of  $(d_s/2) - 1$ . The values of  $d_s$  extracted from the above data are tabulated in table 2. The estimated errors include the variation of slope when the fitting range is varied and not just the error obtained from the least-squares fit.

Table 2. Estimates of  $d_s$  from  $n(\lambda)$  and  $2d_f/d_w$  from  $\lambda_2$ . Column 4 was obtained from data in column 2 and column 5 was obtained from data in column 3.

$d$	$(d_s/2) - 1$	$d_w/d_f$	$d_s$	$2d_f/d_w$
2	$-0.39 \pm 0.01$	$1.606 \pm 0.002$	$1.22 \pm 0.02$	$1.245 \pm 0.001$
3	$-0.36 \pm 0.01$	$1.536 \pm 0.006$	$1.28 \pm 0.02$	$1.302 \pm 0.002$

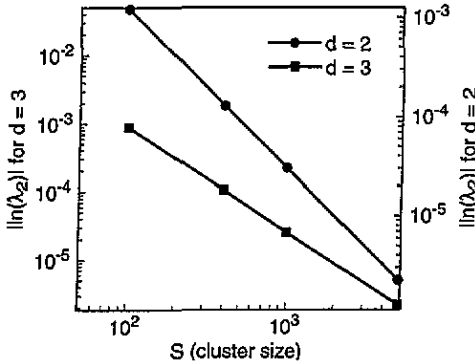


Figure 3. Log-log plot of the second-highest eigenvalue against the size of the cluster.

In figure 3 the second-highest eigenvalue  $\lambda_2$  for the different size clusters is plotted against the size of the cluster on logarithmic scales. The size of the symbols are much larger than the statistical fluctuations. The number of clusters used to find the ensemble average is the same as for the density of eigenvalues. The lines joining the points have correlation coefficients of 0.999 999 indicating excellent power-law relations. The slope of the lines give the exponent ratio  $d_w/d_f$ . The estimated errors associated with the slope are obtained from the least-squares fit. As there are just four data points available for each  $d$ , there might be additional sources of errors which cannot be accounted for with the available data. These estimates of  $d_w/d_f$  are also tabulated in table 2.

The values of  $d_s$  and  $2d_f/d_w$  are calculated from the measured values of  $(d_s/2) - 1$  and  $d_w/d_f$  and are given in columns 4 and 5 of table 2 to make the comparison easier. These estimates are consistent with  $d_s = 2d_f/d_w$  in both two and three dimensions, although the values of  $d_s$  are different from those for ordinary percolation. Therefore we find that Alexander–Orbach relation does hold on loopless percolation cluster in contrast to the Eden tree [5] and DLA [6]. We also note that our numerical result for  $2d_f/d_w$  in  $d = 2$  is consistent with that of [12], where  $d_w$  was determined by a different method (exact enumeration in the time domain). Thus, the loopless percolation model of [12] in two dimensions seems to be in the same universality class as the present model.

### 3. Conclusion

We conclude that the Alexander–Orbach scaling law of equation (3) does not break down in all cases of loopless fractal. On loopless fractals, the random walk experiences more severe trapping than in fractals with loops due to the absence of pathways which connect different branches. This results in higher probability of the walk not exploring the overall fractal nature of the cluster. An example of this occurs in the Eden tree, where the cluster is compact and  $d_f = d$ , and in the DLA. The *smaller* value of  $d_s$  than  $2d_f/d_w$  in these cases

may suggest that the fractal dimension felt by the random walk is *less* than the overall global fractal dimension of the cluster. The branches of these structures are such that they confine the random walker progressively with time. In the case of loopless percolation, although the walk is also confined to a branch, the structure of the branch is such that it does not provide progressive confinement to the random walker, which allows the walk to probe freely the fractal dimension of the branch, which we believe to be the same as that of the entire cluster.

Thus the presence or absence of loops are not the only factors which determine the validity of Alexander–Orbach scaling law for diffusion on fractals, but the intricate structure of the branches themselves are also of fundamental importance.

## References

- [1] Shlesinger M F and West B J (ed) 1984 *Random walks and Their Applications in the Physical and Biological Sciences (AIP Conf. Proc. 109)* (New York: American Institute of Physics)
- [2] Straley J P 1990 *Electrical and Optical Properties of Inhomogeneous Media (AIP Conf. Proc. 40)* ed J C Garland and D B Tanner (New York: American Institute of Physics) and references therein
- [3] Alexander S and Orbach R 1982 *J. Physique Lett.* **43** 625
- [4] Dhar D and Ramaswamy R 1985 *Phys. Rev. Lett.* **54** 1346
- [5] Nakanishi H and Herrmann H 1993 *J. Phys. A: Math. Gen.* **26** 4513
- [6] Jacobs D, Mukherjee S and Nakanishi H 1994 *J. Phys. A: Math. Gen.* **27** 4341
- [7] Sawada Y, Ohata S, Yamazaki M and Honjo H 1984 *Phys. Rev. A* **26** 3557
- [8] Witten T A and Sanders M L 1983 *Phys. Rev. B* **27** 5686
- [9] Witten T A and Sanders M L 1981 *Phys. Rev. Lett.* **47** 1400
- [10] Kolb M, Botet R and Jullien R 1983 *Phys. Rev. Lett.* **47** 1123
- [11] Patterson L 1984 *Phys. Rev. Lett.* **52** 1621
- [12] Tzschichholz F, Bunde A and Havlin S 1989 *Phys. Rev. A* **39** 5470
- [13] Leath P L 1976 *Phys. Rev. B* **14** 5064
- [14] Mukherjee S, Nakanishi H and Fuchs N 1994 *Phys. Rev. E* **49** 5032 and references therein